RESEARCH PAPER

Structural and Antibacterial Properties of Silver Helical Pentagon and L-shaped Nano Sculptured Thin Films

Maryam Malmir

Department of Physics, Faculty of Basic Sciences, Lorestan University, Khorramabad, Lorestan, Iran

ARTICLE INFO

Article History:
Received 19 July 2022
Accepted 14 September 2022
Published 01 October 2022

Keywords:
Antibacterial property
Glancing angle deposition
Sculptured thin films
Silver nanostructure

ABSTRACT

Metallic nanostructures have attracted much attention from scientists due to their numerous applications in many areas of physical sciences, chemical sciences, and life sciences. This study showed that by controlling the shape and dimensions of the nanostructures, surface chemistry and their biocidal and antibacterial activities can be managed. In this study sculptured thin films with L- and helical pentagon-shaped were produced by the glancing angle deposition method. in this method by using an angle between the boat of the sample and substrate and simultaneously rotating the substrate about the azimuthal (or normal) axis, the sculptured nanorods were made, this is the creative physical way to produce nanorods with desired shape and porosity. The morphology and structure properties of these thin films were investigated by X-ray diffraction, atomic force microscopy, and scanning electron microscopy. The antibacterial properties of the films against microorganisms such as Escherichia coli ATCC 8739, Pseudomonas aeruginosa ATCC 10145, Staphylococcus aureus ATCC 25923, Micrococcus luteus ATCC 4698, and Candida albicans PTCC 5027 were studied using the so-called diffusion assay method. Sculptured thin film with HP-shaped showed higher antibacterial activity against all of the studied microorganisms than L-shape one. This may be because of increasing the surface-to-volume ratio and higher surface roughness as well as the high intensity of the Ag(111) orientation. Both of the structures have the most antibacterial effect on the Pseudomonas aeruginosa ATCC 10145 bacteria, the ZOI is 3.90 cm for L-shaped and 5.87 cm for HP-shaped sculptured thin film, respectively.

How to cite this article
Malmir M. Structural and Antibacterial Properties of Silver Helical Pentagon and L-shaped Nano Sculptured Thin Films. J Nanostruct, 2022; 12(4):968-974. DOI: 10.22052/JNS.2022.04.018

INTRODUCTION

Metallic nanostructures have attracted much attention from scientists due to their numerous applications in many areas of physical sciences, chemical sciences, and life sciences. By controlling the shape and dimensions of the nanostructures, surface chemistry, optical properties, and their biocidal activities can be managed. For example, experiments have demonstrated that the plasmon peak depends strongly on the morphology and assembly of the nanoparticles, such as diameter, aspect ratio, and shape [1, 2]. As reported in many studies, the antibacterial activity of metal nanostructures is mainly dependent on their size and shape. for example, Wigginton and coworkers [3], reported that silver nanoparticles attach to the Triptophanase (about 5 nm) in E. coli alter its enzymatic activity and distort its structure [4]. Size-

* *Corresponding Author Email: malmir.m@lu.ac.ir*

dependent interaction of metal nanostructures with gram-negative bacteria has been widely reported, however little is known about the shape dependence of the antibacterial activity of metal nanostructures. Pal et al [5-7] reported that truncated triangular silver nanoplates had a stronger antibacterial activity against E. coli than other shapes such as spherical, rod-shaped nanoparticles. It may be anticipated that a bacterial cell in contact with silver nanoparticles takes in silver ions, which interdicts a respiratory enzyme(s), so cell is damaged. The antibacterial activity of the silver nanoparticles was analyzed and it was found that there was an inverse correlation between the nanostructures' size and their biocidal activity, small particles exhibited higher antimicrobial activity than big particles due to their larger surface-to-volume ratios [8-10]. Reports on the mechanism of inhibitory action of silver ions on microorganisms showed that upon Ag^+ treatment, DNA loses its replication ability, and the expression of ribosomal subunit proteins, as well as some other cellular proteins and enzymes essential to ATP production, become inactivated [11-13]. Also, studies have demonstrated that the reactivity of silver is favored by high-atom-density [14] facets with the bacterial surface [15].

Many scientists use the oblique angle deposition (OAD) method to produce dimensional nanostructures with a high surface area to volume ratio. Glancing angle deposition (GLAD) is another shape of the OAD where substrate rotation is also used. OAD and GLAD [16,17] techniques enable the production of various nanostructures like zig-zags, chevrons, nano-spirals, inclined columns, and branched nano-columns [18-22] for applications of sensing, energy, catalysis, and biomedicine [23].

In this work, we have used this technique and produced silver L-shaped and helical pentagon (HP) sculptured thin films and investigated their structural and antibacterial properties.

MATERIALS AND METHODS

Silver (99.99% purity) L- and HP-shaped nano sculptured thin films were deposited at 75◦ oblique angle deposition on glass (15 × 15mm2 microscope slide) substrates, using resistive evaporation from tungsten boats with an outlet of 6mm diameter at room temperature. An Edwards (Edwards E19 A3) coating plant with a base pressure of 3×10^{-7} mbar and a deposition rate of 2.5A◦ s^{-1} was used. the vapor source (6mm in diameter) behaves like a point source and a 30 cm distance between the evaporation source and the substrate was chosen so a cosine distribution and straight trajectories of the vapor were achieved (i.e., no appreciable scattering due to the large mean free path (∼103–104 cm) occurs). Optical reflection from the reproduced samples was agreed to be within 5%. Different mechanical movements of substrate holders are controlled via an interface to a computer in which the related software is written and installed.

The structure was produced from an initial substrate position for the formation of one arm of the L or HP and then the process were repeated by successive rotation of the substrate holder by 180◦ for one time and 72◦ for ten times for the respective formation of the silver L and HP structures' arms in the anticlockwise direction. The length of each deposited arm is arranged to be about 635 nm and 350 nm for L and HP structures respectively. Considering that the deposition of the films was at 75◦ to the substrate surface normal, using the Tait rule, the height of each arm can be calculated as 635 × sin(90 – 53.2) = 380 nm for the L- shape and 350× sin(90-53.2)=209 nm for the HP-shape. Therefore, the total height of the L shape structure produced in this work with two arms should be equal to ∼760 nanometers and ~2.1 micrometers for an HP-shaped structure with ten arms, This is very close to the measurement from the cross-section of the films in Figure 1. All substrates were ultrasonically cleaned in heated acetone and then ethanol before being mounted on the substrate holder for deposition.

The deposition rate was measured by a quartz crystal deposition rate controller (Sigma Instruments, SQM-160, USA) positioned at almost the same azimuthal angle as that of the substrate and close to that. Field emission electron microscope (FESEM) samples were coated with a very thin layer of gold to prevent the charging effect (FESEM; Hitachi S-4100 SEM, Japan). The surface physical morphology and roughness was obtained by means of atomic force microscope (AFM; NT-MDT SOLVER, with a Si tip of 10nm radius in contact mode) analysis.

Antibacterial activity of the silver nano structures against the *Escherichia coli* ATCC 8739 (E.coli), Pseudomonas aeruginosa ATCC 10145 (Ps. aer), *staphylococcus aureus* ATCC 25923 (*S.aureus)*, Micrococcus luteus ATCC 4698 (M.luteus) and *Candida albicans* PTCC 5027 (*C.albicans)* were studied using the so-called diffusion assay method. Among the bacteria studied, *E coli* and Ps.aer are gram negative, whereas *S.aur and M.loteus are* gram positive and *C.albicans* is a fungal genera [23]. Before experimenting, all films were cleaned with ethanol and acetone and autoclaved at 120 ºC for 15 min. Then they were placed into a sterilized Petri dish and irradiated by a UVC lamp for 30 minutes. The microorganisms were cultured on a nutrient agar plate and incubated at 37 ºC for 24 h, then added in 10 ml saline solution to get the concentration of bacteria 108 colony-forming units per milliliter (CFU/ml) corresponding to the MacFarland scale. 100 µl of the saline solution containing the microorganisms was added to the nutrient agar plate and spread with a sterile cotton swab. Then for the antibacterial test, each thin film was placed onto a cultured nutrient agar plate and incubated at 37 ºC for 24 h. After 24 hours area of inhibition zone of growth was measured.

RESULTS AND DISCUSSIONS

FESEM, AFM and XRD

Fig. 1, shows FESEM images of the surface structure and cross-section of L- and HP-shaped sculptured thin films. Cross-section of the films was obtained by fracturing the substrate that caused the braking of their arms. Hence, in Figure 1(b,d) a proper cross-section of L- and HP-shaped thin films may not be clearly distinguished. The symmetry of the grown L- and HP- shaped on the surface of the films is shown by geometrical shapes (i.e., L shape or HP shape) while the orientation of grown arms is also shown by black arrows. These arrows show the principal axes that the columns grow along their directions. With regard to this observation, we should also point out the high surface diffusion of silver ad atoms because of the rise of substrate temperature from its initial setting during almost 5 hours of deposition, and that these films were grown on bare (unseeded) glass substrates. Therefore, all these parameters/ effects prevent the L- and HP-shaped thin films from growing in a perfectly ordered structure. However, we may claim that these structures are more applicable for industrial or applied works, as preseeding is a costly procedure.

In Fig. 2, 2D and 3D AFM images of silver L- and HP-shaped sculptured thin films are given. The size distributions of the grains of these sculptured thin films were obtained from the 2D AFM images using JMicroVision Code, and the mean and the root mean square (RMS) surface roughness as well as, the average grain sizes are tabulated

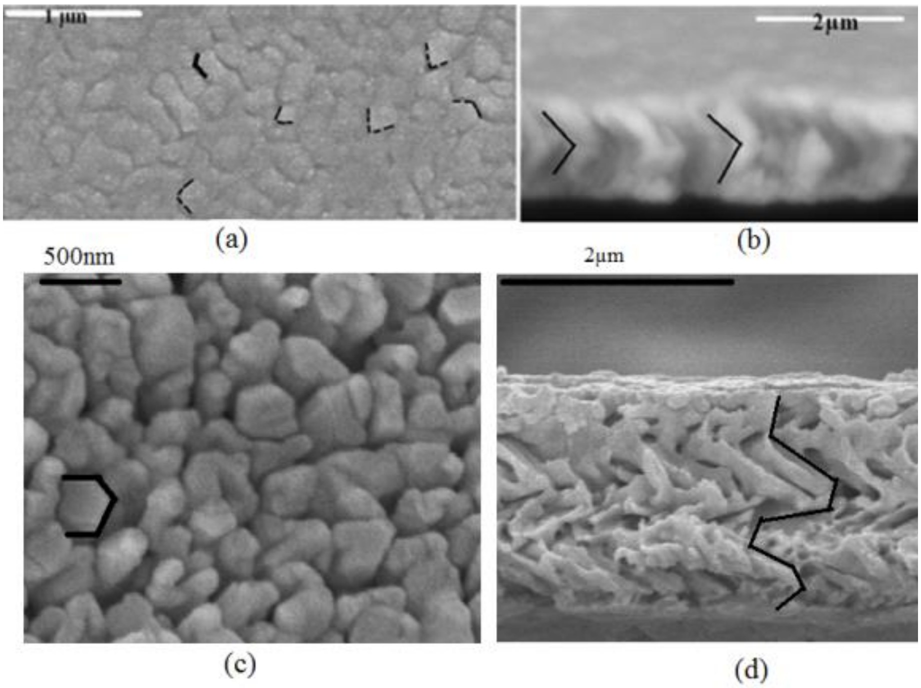

Fig. 1. (a,b), FESEM images of silver L-shaped; (c,d) and for silver HP-shaped sculptured thin films.

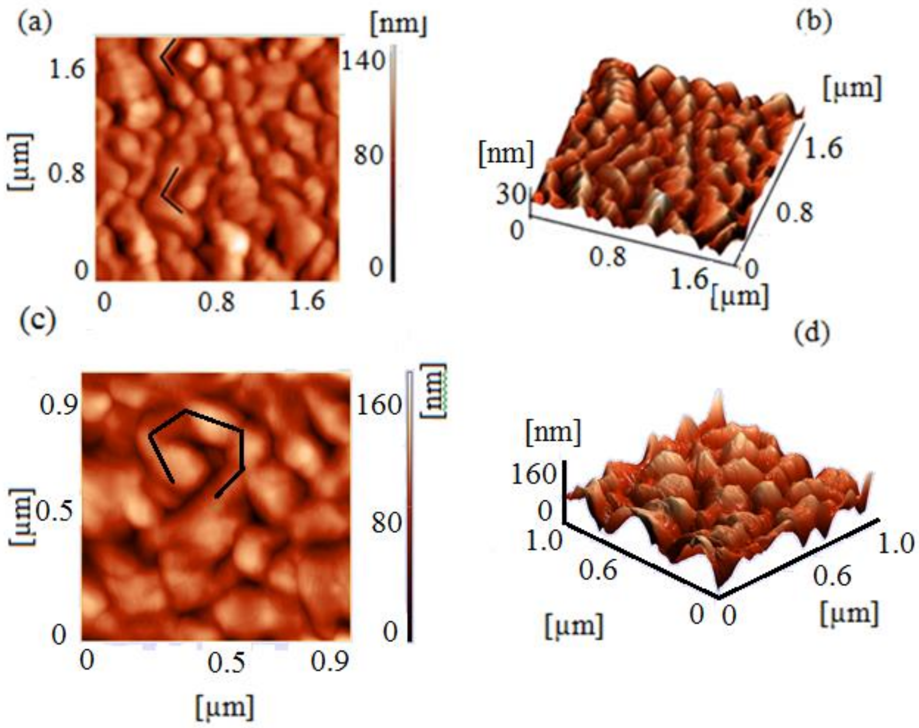

Fig. 2. 2D and 3D AFM images of (a,b) the silver L-shaped and (c,d) silver HP-shaped sculptured thin film.

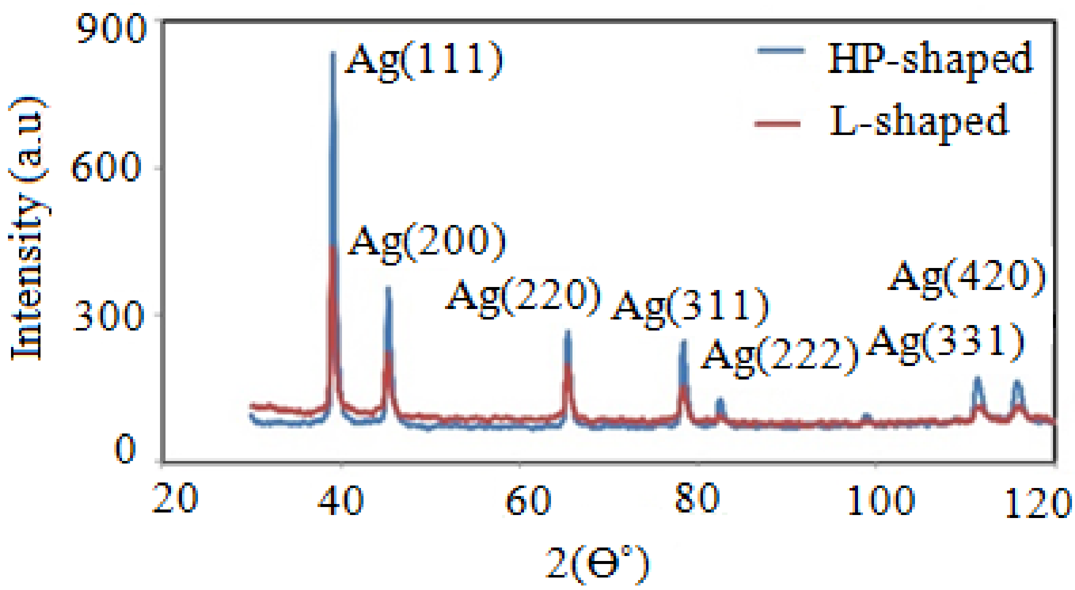

Fig. 3. XRD pattern of two silver nanostructured thin films.

in Table 1. Fig. 3, shows the XRD patterns of the samples. Their crystalline structure is consistent with the JCPDS card No: 04-0783. Crystallite size (coherently diffracting domains), D, was obtained by applying the Scherrer formula [24] to measure the full width at half maximum (FWHM) of the dominant peak of silver sculptured thin films (i.e., Ag(111)). The results with 10% accuracy are given

Table 1. Results of grain size, average surface roughness in the Ag L- and HP-shaped sculptured thin films on glass substrates.

Ag/glass	D_{XRD} [nm]	D_{AFM} [nm]	R_{ave} [nm]
L-shaped	35	192	16
HP-shaped	80	244	18

Fig. 4. typical zone of inhibition (ZOI) for L-shaped (left) and HP(right) sculptured thin films on Petri dish for E. coli ATCC 8739 bacteria, after 24 hours incubation.

Table 2. The ZOI obtained for silver L- and HP-shaped sculptured thin films against different test strains, E. coli, S.aur, C.albicance, M.loteus and Ps. Aer, and compare with previous papers.

	E. coli	S.aur	C.albicance	M.loteus	Ps.aer	
L-shape	2.24 cm	2.31 cm	2.36 cm	2.30 cm	3.90 cm	This work
HP-shape	2.41 cm	2.33 cm	2.42 cm	2.31 cm	5.87 cm	This work
	12.8 mm	------	-------	--------	18 mm	Ref [23]
	2.45 cm					Ref [24]
	1.5 mm				11.3 mm	Ref [25]
	19.5 mm	0.0	-------	------	36 mm	Ref [26]

in Table 1.

Antibacterial property of Ag L- and HP-shaped sculptured thin films

Fig. 4, shows the typical zone of inhibition (ZOI) for L-shaped (a) and helical pentagon (b) thin films on a Petri dish for E. coli ATCC 8739 bacteria, after 24 hours of incubation. ZOI was recorded as the zone of inhibition of the sample (see FIG.4). In Table 2, the ZOI obtained for silver L- and HP-shaped thin films against different test strains, E. coli ATCC 8739, S. aur ATCC 25923 , C. albicance PTCC 5027 and M. loteus ATCC 4698, are compared with each other and with other previously papers [25-28]. It can be concluded that in all of the bacteria cases, the helical pentagon thin films' antibacterial effect dominates the other structure. This may be due to its higher intensity of (111) orientation, as discussed in Section 3.1, and higher surface-to-volume ratio due to the increased number of arms in this film. We also investigated the effect of these nanostructures on Ps.aer as a gram-negative bacteria (such as E.coli), results showed that two structures have the most antibacterial effect on this bacteria with the high ZOI of 3.90 cm for L-shaped thin film and 5.87 cm for helical pentagon thin film (nearly the all of the Petri dish), that they are the biggest ZOI in compare of previous papers. Hence, it may reiterate that by increasing the surface-to-volume ratio and surface roughness of thin films the probability of releasing silver atoms/ions in the medium increases as well as, the Ag(111) facet consists of the maximum number of atoms in the silver structure it should provide the highest antibacterial effect. Therefore, considering the structural and morphological results obtained for our HP- and L-shaped silver thin films, presented in the preceding sections, we expect that our nano-sculptured thin films should show an enhanced antibacterial property compared to a normal film (thin films deposited at a normal incident angle).

CONCLUSION

Sculptured thin film with HP-shaped shows higher antibacterial activity against all of the studied microorganisms than L-shape one. This may because of increasing the surface to volume ratio and surface roughness of this sculptured thin film as well as higher intensity of the Ag(111) orientation with the maximum number of atoms. so probability of releasing silver atoms/ions in the medium increases and the highest antibacterial activity is occured. These structures have the most antibacterial effect on the Pseudomonas aeruginosa ATCC 10145 bacteria, Their ZOI are 3 cm for L-shaped and 6.78 cm for HP-shaped sculptured thin films.

CONFLICT OF INTEREST

The authors declare that there is no conflict of interests regarding the publication of this manuscript.

REFERENCES

1. Alivisatos AP. Semiconductor Clusters, Nanocrystals, and Quantum Dots. Science. 1996;271(5251):933-937.
2. Chen S, Webster S, Czerw R, Xu J, Carroll DL. Morphology Effects on the Optical Properties of Silver Nanoparticles. Journal of Nanoscience and Nanotechnology. 2004;4(3):254-259.
3. Wigginton NS, Titta Ad, Piccapietra F, Dobias J, Nesatyy VJ, Suter MJF, et al. Binding of Silver Nanoparticles to Bacterial Proteins Depends on Surface Modifications and Inhibits Enzymatic Activity. Environmental Science & Technology. 2010;44(6):2163-2168.
4. Méndez-Vilas A, Jódar-Reyes AB, Díaz J, González-Martín ML. Nanoscale aggregation phenomena at the contact line of air-drying pure water droplets on silicon revealed by atomic force microscopy. CAP. 2009;9(1):48-58.
5. Pal S, Tak YK, Song JM. Does the Antibacterial Activity of Silver Nanoparticles Depend on the Shape of the Nanoparticle? A Study of the Gram-Negative Bacterium Escherichia coli. Applied and Environmental Microbiology. 2007;73(6):1712-1720.
6. Wang LL, Sun T, Zhou SY, Shao LQ. The Antibacterial Activities of Ag/Nano-TiO_2 Modified Silicone Elastomer. Acta Physica Polonica A. 2014;125(2):248-250.
7. Altan M, Yildirim H. Comparison of Antibacterial Properties of Nano TiO_2 and ZnO Particle Filled Polymers. Acta Physica Polonica A. 2014;125(2):645-647.
8. Ayala-Núñez NV, Lara Villegas HH, del Carmen Ixtepan Turrent L, Rodríguez Padilla C. Silver Nanoparticles Toxicity and Bactericidal Effect Against Methicillin-Resistant Staphylococcus aureus: Nanoscale Does Matter. Nanobiotechnology. 2009;5(1-4):2-9.
9. Choi O, Hu Z. Size Dependent and Reactive Oxygen Species Related Nanosilver Toxicity to Nitrifying Bacteria. Environmental Science & Technology. 2008;42(12):4583-4588.
10. Martínez-Castañón GA, Niño-Martínez N, Martínez-Gutierrez F, Martínez-Mendoza JR, Ruiz F. Synthesis and antibacterial activity of silver nanoparticles with different sizes. Journal of Nanoparticle Research. 2008;10(8):1343-1348.
11. Feng QL, Wu J, Chen GQ, Cui FZ, Kim TN, Kim JO. A mechanistic study of the antibacterial effect of silver ions onEscherichia coli andStaphylococcus aureus. J Biomed Mater Res. 2000;52(4):662-668.
12. Yamanaka M, Hara K, Kudo J. Bactericidal Actions of a Silver Ion Solution on Escherichia coli, Studied by Energy-Filtering Transmission Electron Microscopy and Proteomic Analysis. Applied and Environmental Microbiology. 2005;71(11):7589-7593.
13. Sondi I, Salopek-Sondi B. Silver nanoparticles as antimicrobial agent: a case study on E. coli as a model for Gram-negative bacteria. Journal of Colloid and Interface Science. 2004;275(1):177-182.
14. Come J, Naguib M, Rozier P, Barsoum MW, Gogotsi Y, Taberna PL, et al. A Non-Aqueous Asymmetric Cell with a Ti_2C-Based Two-Dimensional Negative Electrode. Journal of The Electrochemical Society. 2012;159(8):A1368-A1373.
15. Morones JR, Elechiguerra JL, Camacho A, Holt K, Kouri JB, Ramírez JT, et al. The bactericidal effect of silver nanoparticles. Nanotechnology. 2005;16(10):2346-2353.
16. Robbie K, Brett MJ, Lakhtakia A. Chiral sculptured thin films. Nature. 1996;384(6610):616-616.
17. Robbie K, Brett MJ. Sculptured thin films and glancing angle deposition: Growth mechanics and applications. Journal of Vacuum Science & Technology A: Vacuum, Surfaces, and Films. 1997;15(3):1460-1465.
18. Potočnik J, Nenadović M, Bundaleski N, Jokić B, Mitrić M, Popović M, et al. The influence of thickness on magnetic properties of nanostructured nickel thin films obtained by GLAD technique. Materials Research Bulletin. 2016;84:455-461.
19. Besnard A, Martin N, Millot C, Gavoille J, Salut R. Effect of sputtering pressure on some properties of chromium thin films obliquely deposited. IOP Conference Series: Materials Science and Engineering. 2010;12:012015.
20. Messier RF, Sunal PD, Venugopal VC. Evolution of sculptured thin films. Engineered Nanostructural Films and Materials; 1999/06/30: SPIE; 1999.
21. Suzuki M. Practical applications of thin films nanostructured by shadowing growth. Journal of Nanophotonics. 2013;7(1):073598.
22. Zhou CM, Gall D. The structure of Ta nanopillars grown by glancing angle deposition. Thin Solid Films. 2006;515(3):1223-1227.
23. Rabiei M, Palevicius A, Monshi A, Nasiri S, Vilkauskas A, Janusas G. Comparing Methods for Calculating Nano Crystal Size of Natural Hydroxyapatite Using X-Ray Diffraction. Nanomaterials. 2020;10(9):1627.
24. Cheng Y-H, Chou C-K, Chen C, Cheng S-Y. Critical length of

nanowires for hydrophobic behavior. Chemical Physics Letters. 2004;397(1-3):17-20.
25. Soman S, Ray JG. Silver nanoparticles synthesized using aqueous leaf extract of Ziziphus oenoplia (L.) Mill: Characterization and assessment of antibacterial activity. J Photochem Photobiol B: Biol. 2016;163:391-402.
26. Tailor G, Yadav BL, Chaudhary J, Joshi M, Suvalka C. Green synthesis of silver nanoparticles using Ocimum canum and their anti-bacterial activity. Biochemistry and Biophysics Reports. 2020;24:100848.
27. Raza M, Kanwal Z, Rauf A, Sabri A, Riaz S, Naseem S. Size- and Shape-Dependent Antibacterial Studies of Silver Nanoparticles Synthesized by Wet Chemical Routes. Nanomaterials. 2016;6(4):74.
28. Cyril N, George JB, Joseph L, Raghavamenon AC, V. P S. Assessment of antioxidant, antibacterial and anti-proliferative (lung cancer cell line A549) activities of green synthesized silver nanoparticles from Derris trifoliata. Toxicology Research. 2019;8(2):297-308.